

# Coupled-cluster treatment of molecular strong-field ionization

Thomas-C. Jagau

Department of Chemistry, University of Munich (LMU), D-81377 Munich, Germany

Ionization rates and Stark shifts of  $\text{H}_2$ ,  $\text{CO}$ ,  $\text{O}_2$ ,  $\text{H}_2\text{O}$ , and  $\text{CH}_4$  in static electric fields have been computed with coupled-cluster methods in a basis set of atom-centered Gaussian functions with complex-scaled exponent. Consideration of electron correlation is found to be of great importance even for a qualitatively correct description of the dependence of ionization rates and Stark shifts on the strength and orientation of the external field. The analysis of the second moments of the molecular charge distribution suggests a simple criterion for distinguishing tunnel and barrier suppression ionization in polyatomic molecules.

## I. INTRODUCTION

Molecules exposed to electric or electromagnetic fields of a strength comparable to the internal molecular forces undergo ionization, possibly accompanied by dissociation.<sup>1,2</sup> This process underlies numerous phenomena involving strong fields such as molecular high harmonic generation,<sup>3</sup> laser-induced electron diffraction,<sup>4</sup> and Coulomb explosion.<sup>5</sup> Therefore, the quantitative modeling of molecular strong-field ionization rates is of immediate interest for the interpretation of all experiments in which strong fields are applied.

At low values of Keldysh's adiabaticity parameter,<sup>6</sup> that is, at low frequencies and high intensities, the quasistatic approximation is valid: If the external field varies slowly compared to the inherent time scale of the ionization process, the molecule behaves at every instant as if it was exposed to a static field of the current strength. Ionization occurs because electrons can tunnel through the potential barrier formed by the molecular potential and the external field or at even higher field strengths leave above the barrier. Differences between static and time-dependent fields can be treated in terms of perturbation theory in the low-frequency limit.<sup>7</sup>

Within the quasistatic approximation, the ionization process can be modeled based on static-field ionization rates, but their computation is beyond the reach of quantum-chemical methods for bound states because the interaction with the field turns all bound states into Stark resonances.<sup>8</sup> This is not of practical importance if the external field is weak compared to the internal forces and the response of the molecule can be treated in terms of perturbation theory.<sup>9</sup> However, a perturbative approach is invalid in the quasistatic regime; in Hermitian quantum mechanics, the static-field ionization rate can only be determined from the time-dependent Schrödinger equation.<sup>10</sup>

On the contrary, a time-independent treatment is possible in non-Hermitian quantum mechanics.<sup>8</sup> The ionization rate  $\Gamma$  induced by the external static field  $F$  is associated with the imaginary part of a discrete complex eigenvalue

$$E - i\Gamma/2 \tag{1}$$

of the molecular Hamiltonian. Similarly, the Stark shift  $\Delta E$  can be calculated by comparing the real part of the resonance energy to the field-free case. However, since the Stark reso-

nances are not  $L^2$  integrable, they cannot be treated using quantum chemistry for bound states.

In the case of atomic Stark resonances, complex scaling<sup>11,12</sup> is a handy solution even though the electric field is not dilation analytic. Upon scaling all coordinates in the Hamiltonian by a complex number  $e^{i\theta}$ , the Stark resonance wave function becomes  $L^2$  integrable provided that  $\theta$  exceeds a critical value.<sup>13–16</sup> The eigenvalues of the complex-scaled Hamiltonian can then be computed in analogy to bound states and are interpreted according to Eq. (1).<sup>17–20</sup>

For a molecule in the Born-Oppenheimer approximation, complex scaling is not appropriate.<sup>8</sup> Several alternative complex-variable (CV) techniques have been proposed, notably exterior complex scaling,<sup>21</sup> complex scaling of the Hamiltonian’s matrix elements,<sup>22</sup> the use of a complex-scaled basis,<sup>23</sup> complex-absorbing potentials (CAPs),<sup>24</sup> and reflection-free CAPs.<sup>25</sup> CAPs have evolved to the most popular CV technique for autoionizing resonances (see Ref. 26 for an overview of recent work) and have also been used to investigate Stark resonances induced by time-dependent fields with explicitly time-dependent configuration-interaction singles (TD-CIS).<sup>27–29</sup> On the contrary, electronic-structure calculations in a basis of complex-scaled functions have been carried out only for autoionizing resonances.<sup>30–33</sup>

The computation of molecular static-field ionization rates is a topic of current research; important recent contributions rely on the hybrid antisymmetrized coupled-channels (haCC) approach<sup>34,35</sup> or the weak-field asymptotic theory<sup>36–39</sup> or apply more drastic approximations such as the popular formula by Ammosov, Delone, and Krainov<sup>40</sup> and its extensions.<sup>41,42</sup>

In this work, the method of complex basis functions is applied to molecular Stark resonances induced by static electric fields. The many-body electronic Schrödinger equation is solved within the coupled-cluster singles and doubles (CCSD) approximation<sup>43</sup> and within the CCSD approximation with additional perturbative triples excitations (CCSD(T)).<sup>44,45</sup> The definitions of these methods are the same for all CV techniques and identical to standard CC theory<sup>46</sup> apart from the different metric owing to the non-Hermiticity of the Hamiltonian.<sup>26</sup>

A particular advantage of a CC treatment of molecular Stark resonances is that all ionization channels can be computed as eigenstates of the same Hamiltonian in a biorthogonal representation through the equation-of-motion (EOM) CC formalism.<sup>47,48</sup> Thus, their characterization through Dyson orbitals is straightforward.<sup>49,50</sup> Also, the CC formalism for

molecular properties can be applied to compute moments of the electronic charge distribution, which provides further insight into the ionization process.

The article is organized as follows: Section II covers technical aspects of the computational scheme, while Section III discusses several conceptual aspects of molecular Stark resonances by means of the two-electron systems He and H<sub>2</sub>, for which CCSD is equivalent to full configuration interaction (CI). Section IV presents representative applications to CO, O<sub>2</sub>, H<sub>2</sub>O, and CH<sub>4</sub> and Section V provides some conclusions and an outlook.

## II. COMPUTATIONAL DETAILS

All calculations have been carried out with a development version of the Q-Chem program package, release 5.0.<sup>51</sup> The implementation of Gaussian basis functions with a complex-scaled exponent presented in Ref. 31 is reused. The only piece of code additionally required for Stark resonances is the evaluation of the dipole integrals in the complex-scaled basis, for which the same formulas apply as in the case of real algebra.<sup>52</sup> The implementation of Hartree-Fock (HF) theory in a complex-scaled basis described in Ref. 32 has also been reused with some modifications required due to the differences in the spectrum of the field-including Hamiltonian and its field-free counterpart.<sup>20</sup> Technical aspects of CV-CC methods have been discussed for temporary anions in Refs. 53,54 and apply equally to Stark resonances.

Similar basis sets as those suggested for temporary anions<sup>31</sup> are employed in all calculations. These bases consist of an unscaled part, which is always chosen as cc-pVQZ in this work, and additional diffuse functions at all atoms whose exponents are subject to complex scaling. The latter functions are chosen as the standard diffuse functions from aug-cc-pVQZ plus additional even-tempered s, p, d, and f functions. Details about the basis sets are compiled in the supplementary material. Overall sizes range from 188 functions for H<sub>2</sub> up to 312 functions for CH<sub>4</sub>.

In the employed basis sets, the imaginary part of the field-free energy can grow as large as  $\sim 0.001$  a.u. at some values of the scaling angle  $\theta$  similar to what has been observed in CC calculations of atomic Stark resonances using a complex-scaled Hamiltonian.<sup>20</sup> Therefore, it is essential to correct the resonance energies according to

$$E'_{\text{res}}(F, \theta) = E_{\text{res}}(F, \theta) - E_{\text{res}}(F = 0, \theta) + E_{\text{res}}(F = 0, \theta = 0) \quad (2)$$

as proposed in Ref. 20 and  $\Delta E$  and  $\Gamma$  are then evaluated from  $E'$  at  $\theta_{\text{opt}} = \theta \left| \min(|dE'_{\text{res}}(\theta)/d\theta|) \right.$ .<sup>55</sup> The dependence of  $\theta_{\text{opt}}$  on the quantum-chemical method is weak in most cases so that  $\theta_{\text{opt}}$  from a HF calculation can be used as guess in a subsequent CC calculation. This even holds in cases where HF and CC calculations yield  $\Gamma$  values differing by an order of magnitude. On the contrary, different molecules and field strengths can feature significantly different  $\theta_{\text{opt}}$ . Typical values of  $\theta_{\text{opt}}$  are in the range of 10–25°. In this work,  $\theta_{\text{opt}}$  has been determined to 1°, which is sufficient to evaluate  $\Delta E$  and  $\Gamma$  with a relative precision of < 1% for all cases considered.

### III. RESULTS FOR TWO-ELECTRON SYSTEMS

#### A. Complex-scaled basis functions vs. complex-scaled Hamiltonian

Atomic Stark resonances can be treated by complex scaling. For helium an expansion of the complex-scaled Hamiltonian in the aug-cc-pVQZ basis with additional diffuse s, p, d, and f functions yields ionization rates<sup>20</sup> that agree within 1-2% with reference data obtained by integrating the time-dependent Schrödinger equation<sup>10</sup> or from complex-scaled calculations in a basis of explicitly-correlated two-electron functions.<sup>19</sup>

Representing the Hamiltonian in a partially complex-scaled basis as detailed in Section II constitutes an approximation to exterior complex scaling. As documented in Table S2 in the Supplementary Material, ionization rates for helium obtained with the partially complex-scaled basis consistently overestimate the reference data from explicit complex scaling by about 5% for a wide range of field strengths, while Stark shifts deviate by less than 1%. Considering the great sensitivity of  $\Gamma$  towards truncation of the one-particle basis set and approximations to the many-body treatment,<sup>20</sup> a consistent deviation of 5% appears entirely acceptable.

Notably, at very high ( $F > 0.45$  a.u.) and at low field strengths ( $F < 0.14$  a.u.) the deviations between  $\Gamma$  values become significantly larger. In the low-field limit, this is because  $\Gamma$  itself becomes very small and its dependence on the scaling angle  $\theta$  masks the effect of the field. Whereas complex scaling appears to be applicable to ionization rates as low as  $\sim 10^{-6}$  a.u.,<sup>20</sup> reliable calculations in a complex-scaled basis require somewhat larger  $\Gamma$  values of at least  $\sim 10^{-5}$  a.u. In the high-field limit, better agreement with explicit complex scaling

is observed if more functions in the basis set are scaled. Importantly, however, scaling more basis functions than proposed in Ref. 31 for temporary anions does not reduce the 5% deviation from explicit complex scaling in general.

## B. Potential energy curve of $\text{H}_2$

The electronic Schrödinger equation for  $\text{H}_2$  can be solved exactly within a given basis set for arbitrary HH distances and orientations of the external field with the present implementation. Therefore,  $\text{H}_2$  is the natural first molecular test case. Several representative potential energy curves (PECs) are compiled in Figure 1. The real parts of such complex-valued PECs can be interpreted in analogy to bound states, while the imaginary part yields the ionization rate as a function of the molecular structure.<sup>56</sup> The case with the field being parallel to the molecular axis (upper two panels of Figure 1) has been considered previously<sup>57,58</sup> with the Hamiltonian expressed in a basis of explicitly correlated two-electron functions. Ionization rates from this approach agree within 3% with the present approach for  $F = 0.06\text{--}0.14$  a.u. and  $R(\text{HH})=0.74$  Å (see SI for details).

As Figure 1 illustrates, full CI calculations in a complex-scaled basis set produce smoothly varying energies and ionization rates, at least at the level of precision considered here with  $R(\text{HH})$  varied in steps of  $0.1$  Å. Discontinuities may appear upon zooming in because the optimal scaling angle  $\theta_{\text{opt}}$  varies as a function of the molecular structure. However, this effect seems to be smaller for Stark resonances than for autoionizing resonances, likely because the perturbation of the field-free state by complex scaling can be removed according to Eq. (2) for Stark resonances.

Figure 1 also shows that already a field strength of  $0.14$  a.u. is sufficient to make the minimum in the PEC disappear in the case of a parallel field. Whereas the PEC will always acquire dissociative character eventually if there is a component of the field along the molecular axis, this does not happen if the field is exactly perpendicular. In this latter case, the PEC is just Stark shifted, but retains its field-free shape. In the limit  $R(\text{HH}) \rightarrow \infty$  the Stark shift and the ionization rate converge to twice the values of the hydrogen atom. Interestingly,  $\Gamma$  approaches that limit from above at  $F = 0.06$  a.u. and exhibits a maximum at around  $R(\text{HH}) = 2.0$  Å. This maximum is, however, not to be confused with the maximum in the diabatic ionization rate that occurs at around  $2.8$  Å when the field is parallel to the

molecular axis and is caused by an avoided crossing of two PECs.<sup>57–60</sup> Finally, Figure 1 also illustrates that  $\Gamma$  converges to the ionization rate of the He atom in the limit  $R(\text{HH}) \rightarrow 0$  for both orientations of  $F$ .

### C. Below vs. above barrier ionization

Depending on the strength of the external field, tunnel and barrier suppression ionization can be distinguished. For atoms, the field strength where the transition between the two regimes occurs can be estimated as

$$F_{\text{ABI}} = I_p^2/4 \quad (3)$$

with  $I_p$  as the lowest ionization potential. In molecular strong-field ionization, the same distinction is possible, but there is no simple estimate of the critical field strength akin to Eq. (3). To characterize ionization of diatomic molecules with one electron by a field oriented along the molecular axis, a double-well model can be used,<sup>61</sup> but a generalization to polyatomic molecules with more complicated nuclear configurations and several competing ionization channels does not appear to be straightforward.

Recently, it was demonstrated for various atoms that the transition from tunnel to barrier suppression ionization is accompanied by a marked change in the second moment of the electronic charge distribution, i.e., the spatial extent of the wave function in the direction of the external field.<sup>20</sup> While the resonance wave function becomes more extended with increasing field strength in the tunnel ionization regime, the opposite trend is observed if the ionization takes place above the barrier. The maximum in  $\langle z^2 \rangle(F)$  ( $F$  parallel to  $z$ -axis) coincides very well with the estimate from Eq. (3).<sup>20</sup>

Figure 2 illustrates that similar trends in the second moment are observed for the  $\text{H}_2$  molecule. In each of the four panels, which relate to different orientations of the external field and HH bond lengths, a distinct maximum is observed in the component of the second moment in the direction of the field. If the field is perpendicular to the molecular axis (left two panels of Figure 2), the potential that the outgoing electron needs to overcome is similar to the atomic case. Consequently, the maximum of  $\langle x^2 \rangle$  agrees well with the estimate of  $F_{\text{ABI}}$  from Eq. (3) as documented in Table I. When the field is parallel to the molecular axis

(right two panels of Figure 2), a double-well model is appropriate, but in the case of a many-electron system it is unknown to what degree the charges of the two nuclei are screened. Assuming effective charges of 0.5 a.u. for both nuclei leads to significant deviations of  $F_{\text{ABI}}$  from the maxima of  $\langle z^2 \rangle$  as Table I shows. Better agreement is obtained if one applies the formula for the atomic case (Eq. (3)) assuming that one nucleus is completely screened while the other one is completely unscreened.

The significance of the trends in the second moment lies in the fact that this quantity can be easily computed for polyatomic molecules and thereby offers a clear criterion to distinguish tunnel and barrier suppression ionization in arbitrary many-electron systems without assumptions about their electronic structure. As will be shown in Section IV, a characteristic maximum is also observed for  $\text{O}_2$ ,  $\text{H}_2\text{O}$ , and  $\text{CH}_4$ .

## IV. RESULTS FOR MANY-ELECTRON SYSTEMS

### A. Carbon monoxide

CO has been chosen as the first example of a many-electron system because experimental results are available regarding the angular dependence of the ionization rate<sup>62,63</sup> and an accurate treatment of the electronic structure has proven to be important for a correct description of the ionization process.<sup>34,62-65</sup> Moreover, ionization rates from the haCC approach have been reported in the literature.<sup>34</sup>

Figure 3 shows Stark shifts and ionization rates computed with HF and CCSD at  $F = 0.06$  a.u. and  $F = 0.09$  a.u. as a function of the angle between the external field and the molecular axis. The upper panels illustrate that HF and CCSD disagree whether the Stark shift is larger when the field points towards the carbon atom or towards the oxygen atom. This is not surprising given that electron correlation reverses the sign of the dipole moment of CO. On the contrary, HF and CCSD qualitatively agree about the angular dependence of the ionization rate:  $\Gamma$  is higher when the electron leaves towards the C atom than when it leaves towards the O atom consistent with experimental findings.<sup>62,63</sup> The minimum in  $\Gamma$  occurs at an angle of about  $120^\circ$  ( $F = 0.06$  a.u.) or  $135^\circ$  ( $F = 0.09$  a.u.) with both methods, but HF underestimates the absolute value of  $\Gamma$  by a factor of 3 at  $F = 0.06$  a.u. and still by a factor of 1.5 at  $F = 0.09$  a.u., which is similar to trends in atomic Stark resonances.<sup>20</sup>



The anisotropy of the ionization rate is underestimated at  $F = 0.06$  a.u. within the HF approximation but in qualitative agreement with CCSD at  $F = 0.09$  a.u.

Carbon monoxide has two low-lying ionized states: a  $^2\Sigma$  state and a  $^2\Pi$  state whose energies are obtained with EOM-IP-CCSD at  $F = 0$  as 14.23 eV and 17.16 eV, respectively. The relative energy of the  $^2\Sigma$  state rises or falls by more than 2 eV depending on the orientation of the external field at  $F = 0.09$  a.u., whereas the  $^2\Pi$  state moves by only 0.3 eV at the same field strength. Although the computation of partial widths for decay into specific ionization channels is beyond the present work, their Dyson orbitals provide qualitative insight. Specifically, only the Dyson orbital for the lowest ionized state (depicted as inset in Figure 3) acquires a non-negligible imaginary part at the field strengths considered here, which indicates that decay into this channel dominates the ionization process. The Dyson orbital at  $90^\circ$  also illustrates that the lowest ionized state largely retains its  $\Sigma$  character even though the external field breaks spatial symmetry and  $\Sigma$  and  $\Pi$  can mix.

Figure 3 also shows ionization rates obtained with the haCC approach with 6 cationic states included in the wave function of the resonance. At  $F = 0.06$  a.u., CCSD and haCC(6) qualitatively agree about the ionization rate and its anisotropy, but haCC(6) yields  $\Gamma$  values that are consistently larger ( $4\text{--}8 \cdot 10^{-4}$  a.u., 7–15%). At  $F = 0.09$  a.u., CCSD and haCC(6) agree very well ( $1 \cdot 10^{-4}$  a.u., 2–3%) when the electron leaves towards the O atom ( $180^\circ$ ), but the deviation grows up to 0.002 a.u. (16 %) at  $0^\circ$  so that CCSD predicts a considerably higher anisotropy of  $\Gamma$  than haCC(6).

The discrepancy at  $F = 0.09$  a.u. may reflect the systematic underestimation of ionization rates at high field strengths in haCC due to the ionization channels being treated as bound states.<sup>34</sup> The origin of the discrepancy at  $F = 0.06$  a.u. is less clear and could indicate a shortcoming of the present approach, for example, an insufficient one-electron basis or non-negligible electron correlation beyond the CCSD approximation. Additional calculations at  $\phi = 0^\circ$  and  $\phi = 180^\circ$  ( $F = 0.06$  a.u.) including further diffuse basis functions change  $\Gamma$  by only  $\sim 10^{-5}$  a.u., whereas the (T) correction increases  $\Gamma$  by about 20% and thus overcompensates the difference between CCSD and haCC(6). Noteworthy, going from the quadruple- $\zeta$  basis to a smaller triple- $\zeta$  basis as used for the haCC(6) calculations in Ref. 34 also leads to a 20% increase of  $\Gamma$ .

## B. Dioxygen

Stark shifts and ionization rates of  $\text{O}_2$  computed with HF and CCSD are presented in Figure 4. Electron correlation has only minor impact on  $\Delta E$  (upper left panel), whereas it changes  $\Gamma$  dramatically. As illustrated in the upper right panel, CCSD finds that the ionization rate is at all field strengths higher when the field is oriented parallel to the molecular axis than when it is perpendicular. Also, the ratio  $\Gamma_{\parallel}/\Gamma_{\perp} \approx 1.2\text{--}1.5$  does not vary much with the field strength. On the contrary, at the HF level this ratio is computed to increase substantially from  $< 0.3$  to  $\sim 1$  between  $F = 0.06$  and  $0.16$  a.u., i.e., HF predicts higher  $\Gamma$  for perpendicular orientation. The discrepancy between HF and CCSD at low to medium field strengths is also apparent from the angle-dependent ionization rates shown in the middle panels of Figure 4. At  $F = 0.06$  a.u., HF underestimates  $\Gamma$  by a factor of 3–20 compared to CCSD depending on the orientation, whereas that factor shrinks to 1–2.5 at  $F = 0.10$  a.u. The impact of electron correlation is at all field strengths largest when the field is parallel to the molecular axis. The maximum ionization rate is obtained with CCSD at an angle of  $45^\circ$  at  $F = 0.06$  a.u. and  $0.10$  a.u. consistent with experimental findings,<sup>66</sup> while HF locates the peak in  $\Gamma$  at around  $50^\circ$ .

The lowest-lying state of  $\text{O}_2^+$  ( $^2\Pi_g$ ) is computed by EOM-IP-CCSD to lie at 12.37 eV in the field-free case. Similar to CO, only the Dyson orbital of this state acquires a substantial imaginary part in the presence of the field indicating that formation of this state is the preferred ionization pathway. The relative energy of the  $^2\Pi_g$  state changes by 0.5–0.9 eV at  $F = 0.10$  a.u. depending on the orientation and hence significantly less than the ground state of  $\text{CO}^+$ , which is expected given that  $\text{O}_2$  is nonpolar. It is also noteworthy that the c-norm of the Dyson orbital stays close to 1 at all field strengths and orientations even though HF and CCSD disagree so strongly about  $\Gamma$ .

The lower panels of Figure 4 illustrate the dependence of the second moment of the electronic charge distribution on the field strength. For both parallel and perpendicular orientation of the external field, a characteristic maximum of one component is observed as discussed in Section III C. However, other than for  $\text{H}_2$ , the field strength where that maximum occurs (ca. 0.12 a.u. for both orientations) does not agree with the atomic estimate for the transition between tunnel and above-barrier ionization. Eq. (3) yields  $F_{\text{ABI}} = 0.056$  a.u. for perpendicular orientation, which is clearly wrong given the behavior

of  $\Gamma$  at this field strength and illustrates that Eq. (3) is inapplicable to molecules with many electrons. A value of 0.12 a.u. as suggested by the second moment appears as a better estimate indicating that the tunnel ionization regime extends to a higher field strength than in a hypothetical atom with the same ionization potential.

### C. Water

For a non-linear three-atomic molecule such as water, many more symmetry-unique orientations of the external field exist than for linear molecules. Therefore, the present study has been restricted to four representative orientations: parallel (A) and antiparallel (B) to the molecular axis, perpendicular to the molecular axis in the molecular plane (C), and perpendicular to the molecular plane (D). Figure 5 shows Stark shifts, ionization rates, and second moments as a function of field strength for these four orientations. All quantities were calculated with HF and CCSD and the complex energy (that is,  $\Delta E$  and  $\Gamma$ ) was additionally evaluated at the CCSD(T) level of theory.

The upper left panel of Figure 5 illustrates that electron correlation makes little impact on the Stark shift except for case B where the external field operates against the intrinsic dipole moment of the water molecule. Here, the effect of electron correlation is substantial in that CCSD(T) predicts zero Stark shift at around  $F = 0.13$  a.u., whereas that occurs at  $F = 0.16$  a.u. at the HF level. Likewise, a net dipole moment of zero (that is, a maximum in  $\Delta E(F)$ ) is obtained at around  $F = 0.065$  a.u. with CCSD(T), but at around  $F = 0.078$  a.u. with HF. These discrepancies are somewhat unexpected given that CCSD(T) and HF agree within 7% about the dipole moment of field-free  $\text{H}_2\text{O}$ .

The lower panels of Figure 5 show that HF and CCSD(T) predict the same order of the orientations A–D regarding  $\Gamma$ : Ionization is at all considered field strengths easiest when the field is perpendicular to the molecular plane (case D) and hardest when the field is in plane perpendicular to the molecular axis (case C). The anisotropy parameter  $\Gamma_D/\Gamma_C$  decreases with growing field strength from about 20 at  $F = 0.06$  to below 3 at  $F = 0.14$  a.u. These findings are in line with previous investigations using CAP-augmented TD-CIS.<sup>29</sup> Remarkably,  $\Gamma$  is at all field strengths higher in case B where the field works against the intrinsic dipole moment than in case A where ionization occurs towards the electron-rich side of the molecule. This agrees with a previous investigation based on a single-electron

Schrödinger equation.<sup>67</sup>

Even though electron correlation does not change the order of orientations A–D, it increases absolute values of  $\Gamma$  considerably, in particular at low field strengths. At  $F = 0.06$  a.u., HF and CCSD ionization rates differ by a factor of 3–6 and the (T) correction additionally increases  $\Gamma$  by up to 25%. Those deviations shrink with rising field strength, but even at  $F = 0.14$  a.u., the difference between HF and CCSD is still about 30% and that between CCSD and CCSD(T) about 10%.

From the upper right panel of Figure 5, it is seen that in all four cases A–D, the component of the second moment in the direction of the field exhibits the characteristic peak discussed in Section III C, whereas the other components vary less with the field strength (see SI for details). Consistent with the highest ionization rates for orientation D, the peak is observed at the lowest field strength in this case. Eq. (3) yields  $F_{\text{ABI}} = 0.057$  a.u. using the Stark-shifted lowest ionization potential (13.02 eV; 12.67 eV at  $F = 0$ ) of  $\text{H}_2\text{O}$ , which is in very good agreement with the estimate based on the second moment. This suggests the transition from tunnel to barrier suppression ionization happens in analogy to a hypothetical atom with the same ionization potential for orientation D, while it is shifted to higher field strengths at the other orientations, most strongly in case C, which also features the lowest ionization rates.

#### D. Methane

Figure 6 shows CCSD ionization rates and second moments as a function of field strength for methane. Three orientations of the external field were studied: parallel (A) and antiparallel (B) to a CH bond and bisecting the angle between two CH bonds (C). As the left panel illustrates, the ionization rate depends only weakly on the orientation of the field consistent with the isotropic electron density distribution of methane. A slight preference exists for case B, where the electron leaves the molecule in the direction of a CH bond, but  $\Gamma$  values corresponding to the three different orientations differ only by a factor of 1.2–1.5 in the range  $F = 0.06$ – $0.12$  a.u. (as opposed to up to 20 in the case of  $\text{H}_2\text{O}$ ). HF underestimates  $\Gamma$  by a factor of about 2 at  $F=0.06$  and by 10–20% at  $F = 0.12$  a.u. (see SI for details), which is a relatively small deviation compared to  $\text{H}_2\text{O}$  and especially  $\text{O}_2$ .

The right panel of Figure 6 demonstrates that the component of the second moment in

the direction of the field shows the same characteristic behavior as for the other molecules discussed before. This suggests the onset of the barrier-suppression regime is at a field strength of around 0.08 a.u. for orientation C and at around 0.10 a.u. for the other two orientations. For a hypothetical atom with the ionization potential of CH<sub>4</sub> (14.53 eV at  $F = 0.10$  a.u. and orientation C with EOM-IP-CCSD, 14.43 eV in the field-free case), that onset would be at 0.071 a.u. according to Eq. (3), that is, the tunnel ionization regime is only slightly extended compared to the atomic case.

## V. CONCLUSIONS AND OUTLOOK

This work has demonstrated that CCSD and CCSD(T) calculations in a basis set of atom-centered Gaussian functions with complex-scaled exponent deliver an accurate description of molecular strong-field ionization. Stark shifts and static-field ionization rates are computed as complex eigenvalues of the time-independent many-body Schrödinger equation without invoking any further approximation besides using a finite one-electron basis set and truncating the CC expansion. Key advantages of the proposed method are that it can be applied to polyatomic species with arbitrary molecular structure (subject to the usual constraints about the validity and applicability of CC methods<sup>46</sup>) and that the computation of molecular properties is straightforward.

Results for the two-electron systems He and H<sub>2</sub> are in excellent agreement with reference values as long as the ionization rate is not smaller than ca.  $10^{-5}$  a.u. Selected applications to many-electron systems illustrate the huge impact of electron correlation on the ionization rate, especially in the tunnel ionization regime. For example, HF and CCSD ionization rates of O<sub>2</sub> differ by a factor of up to 20 at low field strengths and the methods also disagree about the orientation of the external field at which the ionization rate is highest. For the polar molecules CO and H<sub>2</sub>O, electron correlation also makes a significant impact on the Stark shift.

A distinct maximum in the component of the second moment of the electronic charge distribution in the direction of the external field is observed for all considered molecules (H<sub>2</sub>, O<sub>2</sub>, H<sub>2</sub>O, CH<sub>4</sub>) at a certain field strength. This peak can be associated with the transition from tunnel to barrier suppression ionization by analogy with atomic Stark resonances. The position of the peak can vary substantially with the orientation; in particular, it is shifted

to higher field strengths at orientations where ionization is suppressed.

While the results reported here are very encouraging, it is also clear that further work along several lines is needed: First, because of the extreme basis-set requirements, the CC treatment presented in this work is suitable only for small molecules. This makes the implementation of more cost-effective methods desirable in order to study strong-field ionization of larger molecules. Second, the computation of partial widths of individual channels needs to be enabled for a more detailed characterization of the ionization process. Third, an extension of the current method to Stark resonances in time-dependent fields appears worthwhile to pursue.

## VI. SUPPLEMENTARY MATERIAL

See supplementary material for details about the basis sets and molecular structures, numerical results corresponding to Figures 1–6 and additional results.

## VII. ACKNOWLEDGMENTS

This work has been supported by the Emmy Noether program of the Deutsche Forschungsgemeinschaft (grant JA 2794/1-1).

## VIII. TABLES

TABLE I. Estimates of the critical field strength at which the transition from tunnel to barrier suppression ionization occurs in the  $\text{H}_2$  molecule.

orientation	$R(\text{HH})/\text{\AA}$	$I_p/\text{eV}^a$	$F_{\text{ABI}}/\text{a.u.}^b$
perpendicular	0.74	17.00	0.098
perpendicular	1.40	13.73	0.064
parallel	0.74	17.14	0.095
parallel	1.40	13.70	0.058

<sup>a</sup> Computed with EOMIP-CCSD at  $F=0.10$  a.u. ( $R(\text{HH})=0.74$  \AA) and  $F=0.06$  a.u. ( $R(\text{HH})=1.40$  \AA).

<sup>b</sup> Calculated according to Eq. (3) for perpendicular orientation and using a double-well model for parallel orientation.

## IX. FIGURES

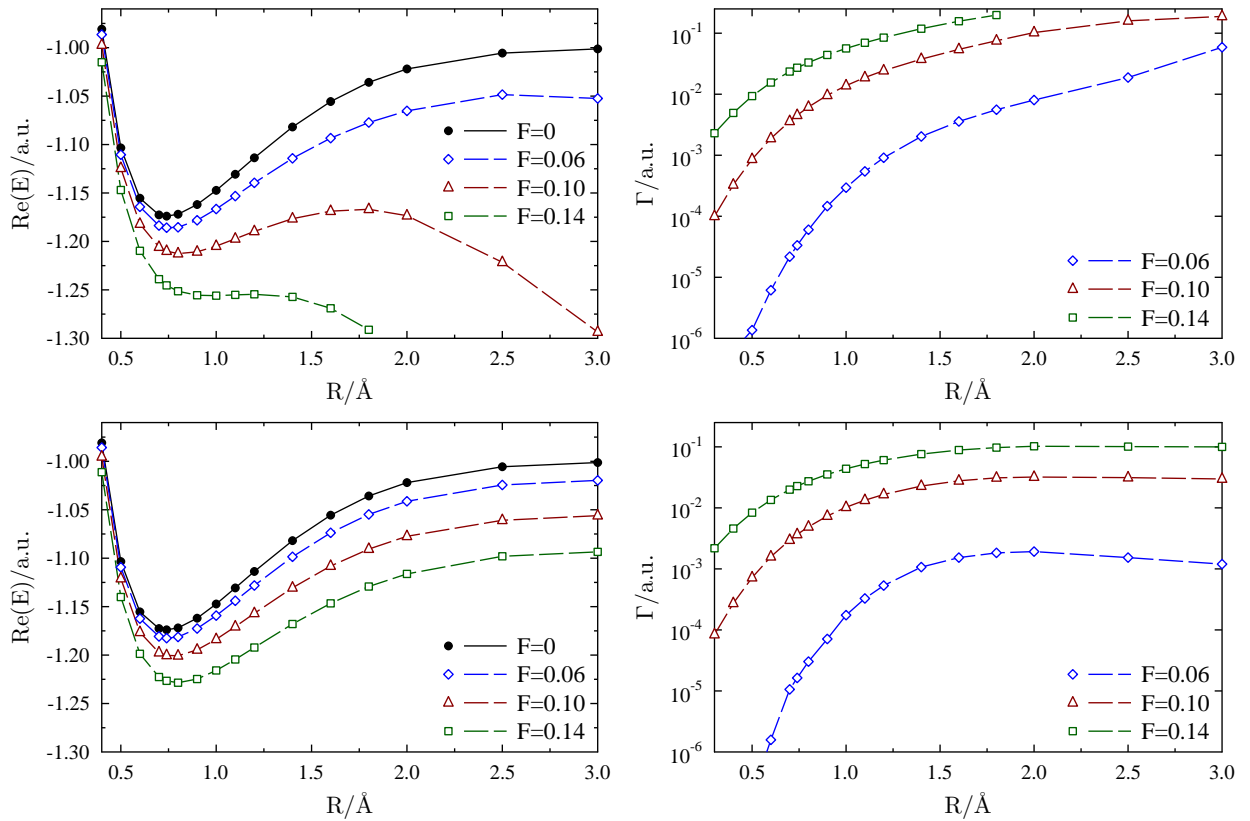


FIG. 1. Potential energy curve (left) and ionization rate (right) of  $\text{H}_2$  at different field strengths oriented parallel (upper panels) or perpendicular (lower panels) to the molecular axis computed at the full CI level of theory using a modified aug-cc-pVQZ basis set.

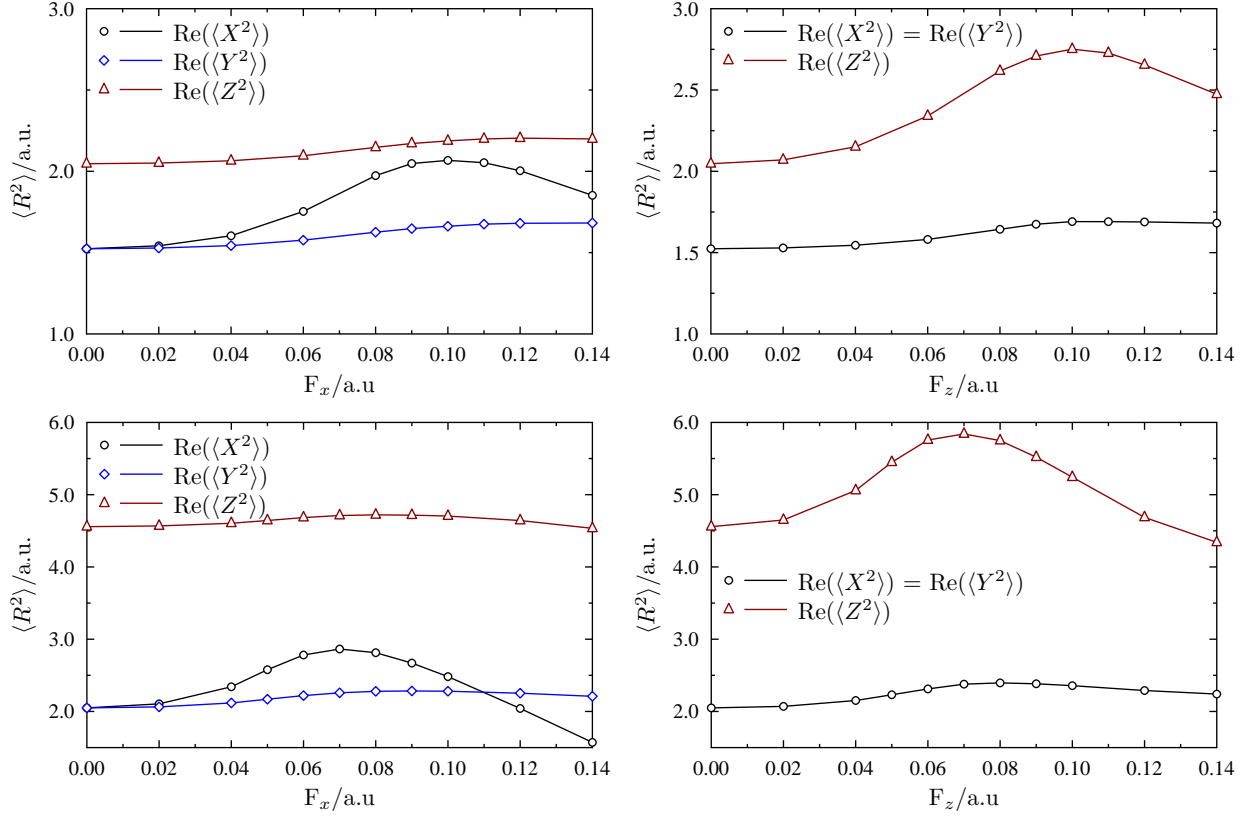


FIG. 2. Real parts of second moments  $\langle R^2 \rangle$  for  $\text{H}_2$  computed at the full CI level of theory using a modified aug-cc-pVQZ basis set. The field is oriented either perpendicular (left panels) or parallel (right panels) to the molecular axis (=z-axis). The HH distance is 0.74 Å (upper panels) or 1.40 Å (lower panels).



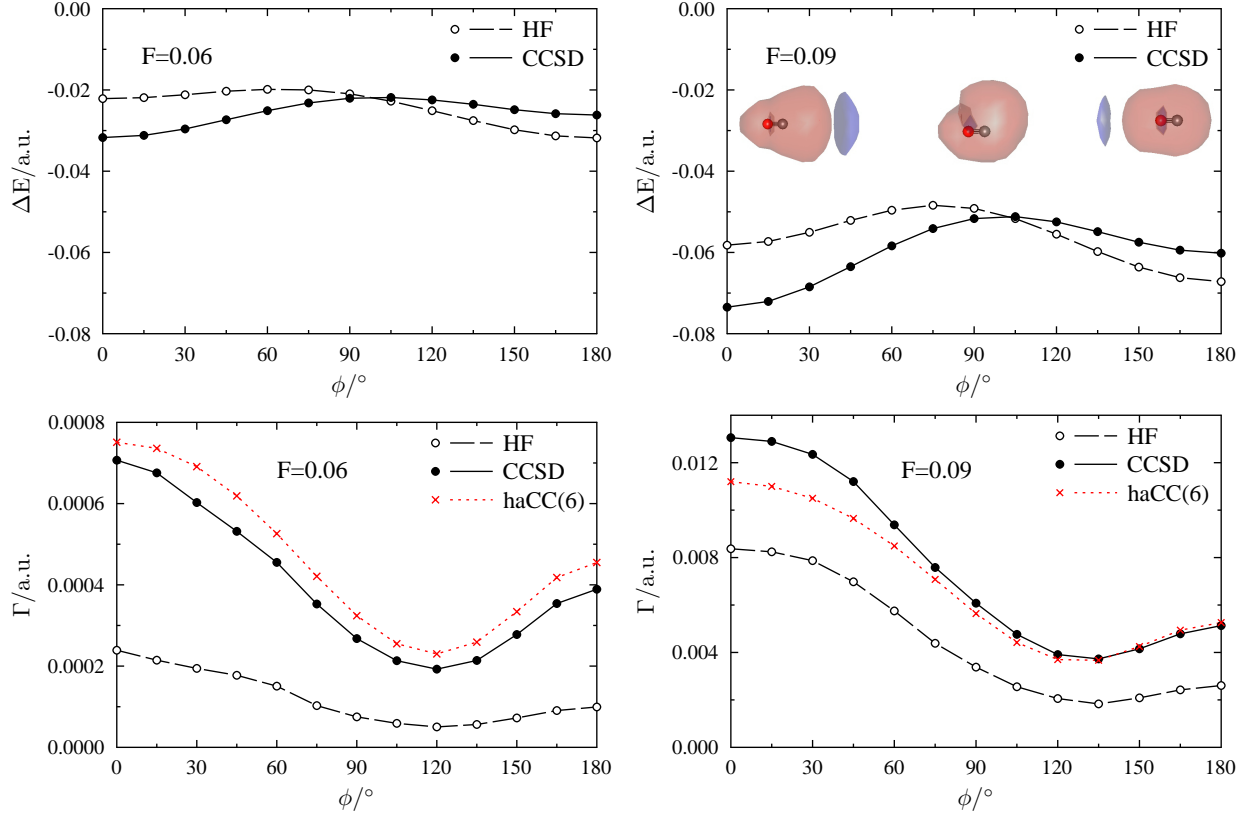


FIG. 3. Angle dependent Stark shifts  $\Delta E$  (upper panels) and ionization rates  $\Gamma$  (lower panels) of CO at field strengths of  $F = 0.06$  a.u. (left) and  $F = 0.09$  a.u. (right) computed at the HF and CCSD levels of theory using a modified aug-cc-pVQZ basis set. Ionization rates from Ref. 34 obtained with the haCC(6) approach are also shown.  $\phi = 0^\circ$  corresponds to the field pointing from C to O. The real part of the Dyson orbital for decay into the ground state of  $\text{CO}^+$  is shown as inset at  $0^\circ$ ,  $90^\circ$ , and  $180^\circ$ .

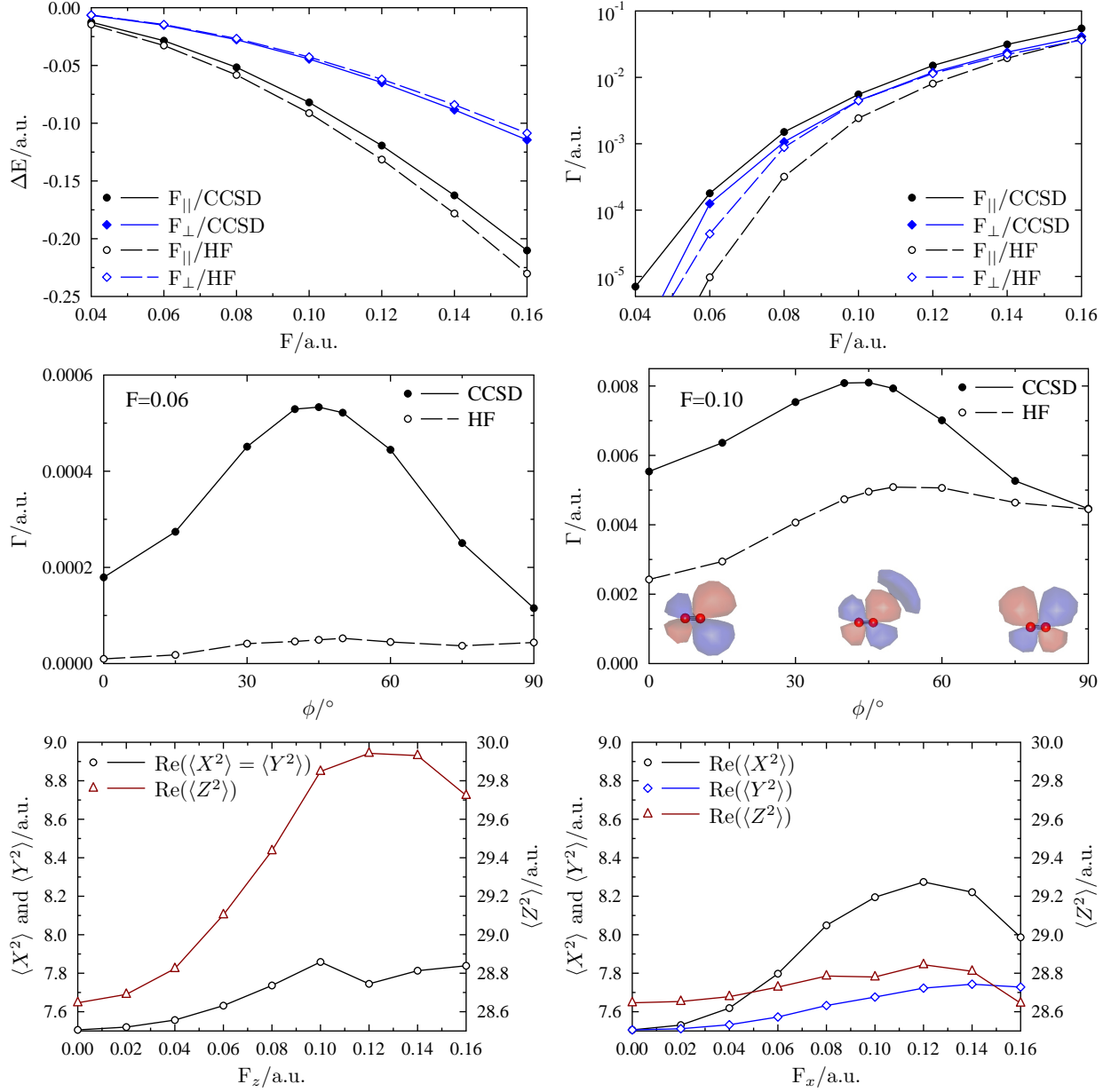


FIG. 4. Strong-field ionization of  $O_2$  studied at the HF and CCSD levels of theory using a modified aug-cc-pVQZ basis set. Upper panels: Stark shifts  $\Delta E$  (left) and ionization rates  $\Gamma$  (right) as a function of field strength  $F$ . The field is oriented either parallel ( $\parallel$ ) or perpendicular ( $\perp$ ) to the molecular axis ( $=z$ -axis). Middle panels: Angle dependent ionization rates at  $F = 0.06$  a.u. (left) and  $F = 0.10$  a.u. (right).  $\phi = 0^\circ$  corresponds to the field oriented parallel to the  $z$ -axis. The real part of the Dyson orbital for decay into the ground state of  $O_2^+$  is shown as inset at  $0^\circ$ ,  $45^\circ$ , and  $90^\circ$ . Lower panels: Real parts of the components of the second moment. The field is oriented either parallel (left panel) or perpendicular (right panel) to the  $z$ -axis.

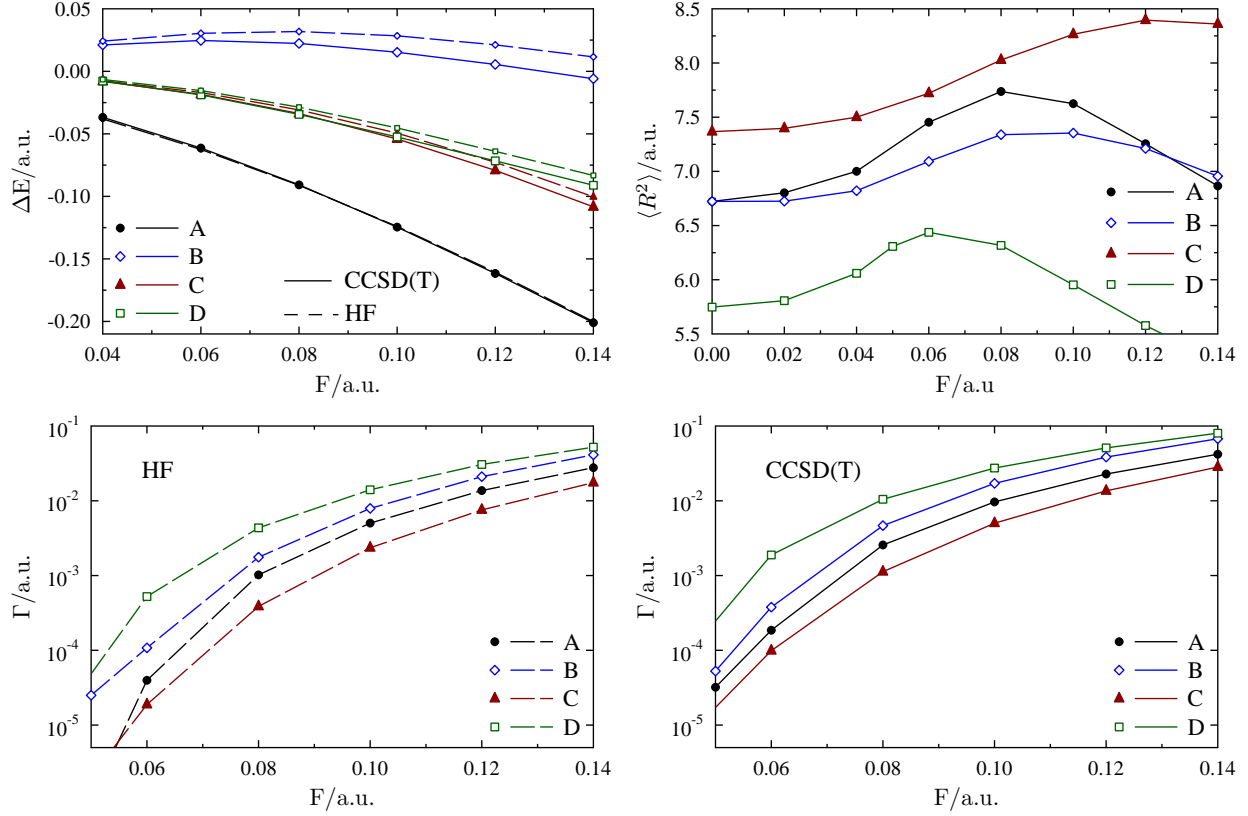


FIG. 5. Strong-field ionization of  $H_2O$  studied at the HF, CCSD, and CCSD(T) levels of theory using a modified aug-cc-pVQZ basis set. Upper left panel: Stark shifts  $\Delta E$  as a function of field strength. Upper right panel: Real part of the component of the second moment in the direction of the external field as a function of field strength. Lower panels: Ionization rates  $\Gamma$  as a function of field strength. The field is oriented as follows:

- A — along the molecular axis ( $=z$ -axis), away from the oxygen atom,
- B — along the molecular axis ( $=z$ -axis), towards the oxygen atom,
- C — perpendicular to the molecular axis in the molecular plane ( $=$  along the  $y$ -axis),
- D — perpendicular to the molecular plane ( $=$  along the  $x$ -axis)

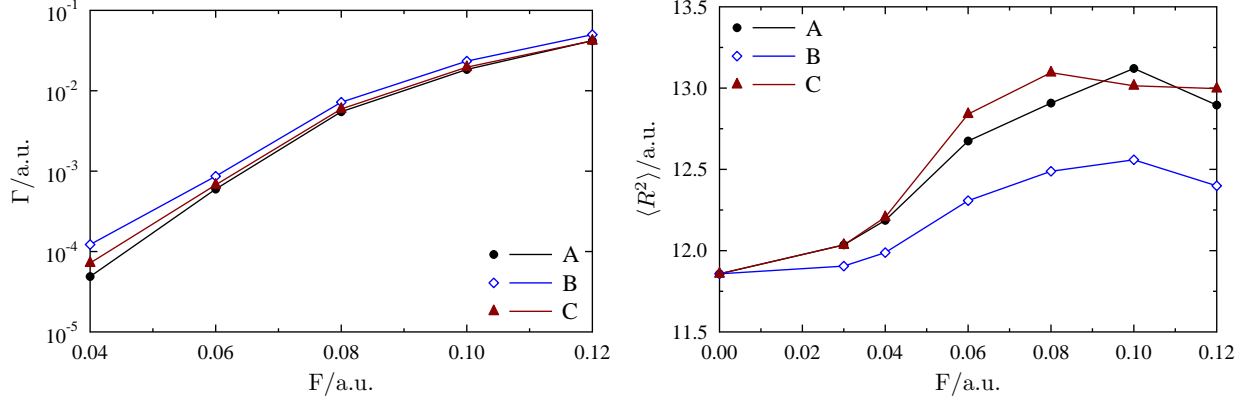


FIG. 6. Strong-field ionization of  $\text{CH}_4$  studied at the CCSD level of theory using a modified aug-cc-pVQZ basis set. Left panel: Ionization rates  $\Gamma$  of  $\text{CH}_4$  as a function of field strength. Right panel: Real part of the component of the second moment in the direction of the external field as a function of field strength. The field is oriented as follows:

- A — along a CH bond towards the hydrogen atom (= along the vector  $(0 \ -\sqrt{2} \ -1)$ ),
- B — along a CH bond towards the carbon atom (= along the vector  $(0 \ \sqrt{2} \ 1)$ ),
- C — bisecting the angle between two CH bonds (= along the  $z$ -axis)

## X. REFERENCES

---

- <sup>1</sup> A. Scrinzi, M.Yu. Ivanov, R. Kienberger, and D.M. Villeneuve, *J. Phys. B* **39**, R1 (2006).
- <sup>2</sup> M. Lein, *J. Phys. B* **40**, R135 (2007).
- <sup>3</sup> J.P. Marangos, *J. Phys. B* **49**, 132001 (2016).
- <sup>4</sup> T. Zuo, A.D. Bandrauk, and P.B. Corkum, *Chem. Phys. Lett.* **259**, 313 (1996).
- <sup>5</sup> Z. Vager, R. Naaman, and E.P. Kanter, *Science* **244**, 426 (1989).
- <sup>6</sup> L.V. Keldysh, *Sov. Phys. JETP* **20**, 1307 (1965).
- <sup>7</sup> H. Martiskainen and N. Moiseyev, *J. Chem. Phys.* **147**, 224101 (2017).
- <sup>8</sup> N. Moiseyev, *Non-Hermitian Quantum Mechanics* (Cambridge University Press, Cambridge, UK, 2011).
- <sup>9</sup> T. Helgaker, S. Coriani, P. Jørgensen, K. Kristensen, J. Olsen, and K. Ruud, *Chem. Rev.* **112**, 543 (2012).
- <sup>10</sup> J.S. Parker, G.S.J. Armstrong, M. Boca, and K.T. Taylor, *J. Phys. B.* **42**, 134011 (2009).
- <sup>11</sup> J. Aguilar and J.M. Combes, *Commun. Math. Phys.* **22**, 269 (1971).
- <sup>12</sup> E. Balslev and J.M. Combes, *Commun. Math. Phys.* **22**, 280 (1971).
- <sup>13</sup> I.W. Herbst and B. Simon, *Phys. Rev. Lett.* **41**, 67 (1978).
- <sup>14</sup> I.W. Herbst, *Commun. Math. Phys.* **64**, 279 (1979).
- <sup>15</sup> I.W. Herbst and B. Simon, *Commun. Math. Phys.* **80**, 181 (1981).
- <sup>16</sup> C.A. Nicolaides and S.I. Themelis, *Phys. Rev. A* **45**, 349 (1992).
- <sup>17</sup> W.P. Reinhardt, *Int. J. Quantum Chem.* **10**, 359 (1976).
- <sup>18</sup> C.A. Nicolaides and S.I. Themelis, *Phys. Rev. A* **47**, 3122 (1993).
- <sup>19</sup> A. Scrinzi, M. Geissler, and T. Brabec, *Phys. Rev. A* **83**, 706 (1999).
- <sup>20</sup> T.-C. Jagau, *J. Chem. Phys.* **145**, 204115 (2016).
- <sup>21</sup> B. Simon, *Phys. Lett. A* **71**, 211 (1979).
- <sup>22</sup> N. Moiseyev and C. Corcoran, *Phys. Rev. A* **20**, 814 (1979).
- <sup>23</sup> C.W. McCurdy and T. Rescigno, *Phys. Rev. Lett.* **41**, 1364 (1978).
- <sup>24</sup> U.V. Riss and H.-D. Meyer, *J. Phys. B* **26**, 4503 (1993).
- <sup>25</sup> N. Moiseyev, *J. Phys. B* **31**, 1431 (1998).

- <sup>26</sup> T.-C. Jagau, K.B. Bravaya, and A.I. Krylov, *Annu. Rev. Phys. Chem.* **68**, 525 (2017).
- <sup>27</sup> P. Krause, J.A. Sonk, and H.B. Schlegel, *J. Chem. Phys.* **140**, 174113 (2014).
- <sup>28</sup> P. Krause and H.B. Schlegel, *J. Phys. Chem. Lett.* **6**, 2140 (2015).
- <sup>29</sup> P. Krause and H.B. Schlegel, *J. Phys. Chem. A* **119**, 10212 (2015).
- <sup>30</sup> M. Honigmann, R.J. Buenker, and H.-P. Liebermann, *J. Chem. Phys.* **125**, 234304 (2006).
- <sup>31</sup> A. F. White, M. Head-Gordon, and C. W. McCurdy, *J. Chem. Phys.* **142**, 054103 (2015).
- <sup>32</sup> A. F. White, C. W. McCurdy, and M. Head-Gordon, *J. Chem. Phys.* **143**, 074103 (2015).
- <sup>33</sup> A. F. White, E. Epifanovsky, C. W. McCurdy, and M. Head-Gordon, *J. Chem. Phys.* **146**, 234107 (2017).
- <sup>34</sup> V.P. Majety and A. Scrinzi, *J. Phys. B* **48**, 245603 (2015).
- <sup>35</sup> V.P. Majety, A. Zielinski, and A. Scrinzi, *New J. Phys.* **17**, 063002 (2015).
- <sup>36</sup> O.I. Tolstikhin, L.B. Madsen, and T. Morishita, *Phys. Rev. A* **89**, 013421 (2014).
- <sup>37</sup> L.B. Madsen, F. Jensen, O.I. Tolstikhin, and T. Morishita, *Phys. Rev. A* **89**, 033412 (2014).
- <sup>38</sup> S.G. Walt, N.B. Ram, A. von Conta, O.I. Tolstikhin, L.B. Madsen, F. Jensen, and H.J. Wörner, *J. Phys. Chem. A* **119**, 11772 (2015).
- <sup>39</sup> L. Yue, S. Bauch, and L.B. Madsen, *Phys. Rev. A* **96**, 043408 (2017).
- <sup>40</sup> M. Ammosov, N. Delone, and V. Krainov, *Sov. Phys. JETP* **64**, 1191 (1986).
- <sup>41</sup> X.M. Tong, Z.X. Zhao, and C.D. Lin, *Phys. Rev. A* **66**, 033402 (2002).
- <sup>42</sup> X.M. Tong and C.D. Lin, *J. Phys. B* **38**, 2593 (2005).
- <sup>43</sup> G.D. Purvis and R.J. Bartlett, *J. Chem. Phys.* **76**, 1910 (1982).
- <sup>44</sup> K. Raghavachari, G.W. Trucks, J.A. Pople, and M. Head-Gordon, *Chem. Phys. Lett.* **157**, 479 (1989).
- <sup>45</sup> R.J. Bartlett, J.D. Watts, S.A. Kucharski, and J. Noga, *Chem. Phys. Lett.* **165**, 513 (1990).
- <sup>46</sup> I. Shavitt and R.J. Bartlett, *Many-Body Methods in Chemistry and Physics: MBPT and Coupled-Cluster Theory* (Cambridge University Press, Cambridge, UK, 2009).
- <sup>47</sup> A.I. Krylov, *Annu. Rev. Phys. Chem.* **59**, 433 (2008).
- <sup>48</sup> K. Sneskov and O. Christiansen, *WIREs Comput. Mol. Sci.* **2**, 566 (2012).
- <sup>49</sup> C.M. Oana and A.I. Krylov, *J. Chem. Phys.* **127**, 234106 (2007).
- <sup>50</sup> T.-C. Jagau and A.I. Krylov, *J. Chem. Phys.* **144**, 054113 (2016).
- <sup>51</sup> Y. Shao, Z. Gan, E. Epifanovsky, A.T.B. Gilbert, M. Wormit, *et al.*, *Mol. Phys.* **113**, 184 (2015).
- <sup>52</sup> O. Matsuoka, *Int. J. Quantum Chem.* **5**, 1 (1971).

- <sup>53</sup> K.B. Bravaya, D. Zuev, E. Epifanovsky, and A.I. Krylov, *J. Chem. Phys.* **138**, 124106 (2013).
- <sup>54</sup> D. Zuev, T.-C. Jagau, K.B. Bravaya, E. Epifanovsky, Y. Shao, E. Sundstrom, M. Head-Gordon, and A.I. Krylov, *J. Chem. Phys.* **141**, 024102 (2014).
- <sup>55</sup> N. Moiseyev, P.R. Certain, and F. Weinhold, *Mol. Phys.* **36**, 1613 (1978).
- <sup>56</sup> N. Moiseyev, *J. Chem. Phys.* **146**, 024101 (2017).
- <sup>57</sup> A. Saenz, *Phys. Rev. A* **61**, 051402 (2000).
- <sup>58</sup> A. Saenz, *Phys. Rev. A* **66**, 063407 (2002).
- <sup>59</sup> T. Seideman, M.Y. Ivanov, and P.B. Corkum, *Phys. Rev. Lett.* **75**, 2819 (1995).
- <sup>60</sup> T. Zuo and A.D. Bandrauk, *Phys. Rev. A* **52**, R2511 (1995).
- <sup>61</sup> A.D. Bandrauk and F. Légaré, “Enhanced Ionization of Molecules in Intense Laser Fields”, in *Progress in Ultrafast Intense Laser Science VIII*, edited by K. Yamanouchi, M. Nisoli, W.T. Hill (Springer-Verlag, Berlin/Heidelberg, 2012).
- <sup>62</sup> H. Li, D. Ray, S. De, I. Znakovskaya, W. Cao, G. Laurent, Z. Wang, M.F. Kling, A.T. Le, and C.L. Cocke, *Phys. Rev. A* **84**, 043429 (2011).
- <sup>63</sup> J. Wu, L.P.H. Schmidt, M. Kunitski, M. Meckel, S. Voss, H. Sann, H. Kim, T. Jahnke, A. Czasch, and R. Dörner, *Phys. Rev. Lett.* **108**, 183001 (2012).
- <sup>64</sup> B. Zhang, J. Yuan, and Z. Zhao, *Phys. Rev. Lett.* **111**, 163001 (2013).
- <sup>65</sup> M.D. Śpiewanowski and L.B. Madsen, *Phys. Rev. A* **91**, 043406 (2015).
- <sup>66</sup> D. Pavičić, K.F. Lee, D.M. Rayner, P.B. Corkum, and D.M. Villeneuve, *Phys. Rev. Lett.* **98**, 243001 (2007).
- <sup>67</sup> S.A. Laso and M. Horbatsch, *J. Phys. B* **50**, 225001 (2017).